Magnetic properties of chromium doped rare earth manganites $Ln_{0.5}Ca_{0.5}Mn_{1-x}Cr_xO_3$ (Ln=Pr, Nd, Sm and $0.05 \leqslant x \leqslant 0.10$) by soft x-ray magnetic circular dichroism

O. Toulemonde,[a] F. Studer, A. Barnabé, and B. Raveau
Laboratoire CRISMAT, UMR 6508 associée au CNRS, ISMRA, boulevard Maréchal Juin, 14050 Caen Cedex, France

J. B. Goedkoop[b]
ESRF, BP 220, 38043 Grenoble Cedex, France

(Received 23 November 1998; accepted for publication 24 May 1999)

Soft-x-ray magnetic circular dichroism (SXMCD) at Mn, Cr $L_{2,3}$ and Ln $M_{4,5}$ edges of $Ln_{0.5}Ca_{0.5}Mn_{1-x}Cr_xO_3$ (Ln=Pr, Nd, Sm and $0.05 \leqslant x \leqslant 0.10$) bulk polycrystalline samples have been performed at $T=20$ K below the ferromagnetic Curie temperature. We show the existence of magnetic sublattice on each of the probed cations. Chromium cations order at low temperature antiparallel to the manganese subnetwork and rare earth cations likely exhibit a sperimagnetic ordering. These results are compared with magnetization measurements and a tentative correlation with magnetoresistance properties is discussed. This work also demonstrates that SXMCD can probe element and site specific magnetic properties of multicomponent systems. © *1999 American Institute of Physics.* [S0021-8979(99)02917-5]

I. INTRODUCTION

The soft x-ray magnetic circular dichroism (SXMCD) has now become a basic tool to investigate the magnetic properties of solids.[1] The SXMCD observed in near-edge core absorption processes is related to the magnetic moment of the photoexcited atom when the core electron is promoted into final states that are responsible for ferro- or ferrimagnetic properties of the system. SXMCD benefits also from the double selectivity of the x-ray absorption spectroscopy (XAS): it is sensitive to the chemical species of the absorbing atom and to the symmetry of the unoccupied electronic states probed by the photoelectron taking into account the electric dipole selection rules.

In this work, we used SXMCD to investigate the magnetic properties of chromium doped rare earth manganites $Ln_{0.5}Ca_{0.5}Mn_{1-x}Cr_xO_3$ (Ln=Pr, Nd, Sm)[2] by determining the element specific magnetic ordering.

Extensive studies of the manganese oxide perovskites $Ln_{1-x}A_xMnO_3$ (Ln=Re; A=Ca, Sr, Ba or Pb) were carried out especially in the past 5 years after the discovery of giant or even colossal magnetoresistance (CMR) in these compounds.[3] Doping the $LnMnO_3$ antiferromagnetic insulator by alkaline–earth cation leads to mixed Mn^{3+}/Mn^{4+} valency, ferromagnetism, and metallic conductivity, which could be due to hole doping in a $2p$ oxygen band. This was explained within the double-exchange mechanism.[4] However, the double-exchange model, considering primarily the spin-dependent hopping mechanism, turns out to be insufficient to explain the insulator behavior above T_c. Thus, a polaronic type model,[5] based on the possible existence of dynamic Jahn–Teller distortion of the MnO_6 octahedra, was proposed to explain such CMR properties.

Up to now, neutron studies of these manganites showing lattice evolution and variation of isotropic Debye–Waller factors at T_c,[6,7] extended x-ray absorption fine structure studies showing changes in the Debye–Waller factor at T_c,[8] and XAS studies at the O K[9] and Mn $L_{2,3}$ edges[10] showing changes in the local distortion of the MnO_6 octahedra support strongly this small polaron model which includes the Jahn–Teller distortion.

Small angle neutron scattering[11] and calorimetric measurements[12] were also interpreted as evidence of the formation of magnetic polarons. At high temperature, an activated conduction with a Curie–Weiss behavior of the magnetization would be observed whereas, just above T_c, the conductivity would follow Mott's variable range hopping model and spin-cluster formation would be responsible for magnetization behavior.[12] Below T_c, Park *et al.* have recently observed a spin dependence of the Fermi level by high resolution spin resolved photoemission on $La_{0.7}Sr_{0.3}MnO_3$ thin films.[13] These results are in agreement with spin polarized band structure calculations,[14] which strongly suggest a semimetallic behavior for the lanthanum manganites below T_c.

Here, we present a direct investigation of the local magnetic moment carried by manganese, chromium, and rare earth cations probe at $L_{2,3}$ edges for transition elements and $M_{4/5}$ edges for rare earth elements. A correlation between magnetization measurements and SXMCD signals is proposed in connection with magnetoresistance properties.

II. EXPERIMENT

The chromium doped rare earth manganites $Ln_{0.5}Ca_{0.5}Mn_{1-x}Cr_xO_3$ (Ln=Pr, Nd, Sm) were prepared in

[a]Author to whom correspondence should be addressed; electronic mail: oliver.toulemonde@ismra.fr
[b]Present address: Faculty of Mathematics, Computer Science, Physics and Astronomy, University of Amsterdam, Valckenierstraat 65, NL 1018 XE, Amsterdam.

the form of sintered pellets following a classical method of solid state chemistry. Thorough mixtures of oxides $CaCO_3$, Cr_2O_3, Mn_2O_3, Nd_2O_3, Sm_2O_3, or Pr_6O_{11} were first heated in air at 950 °C for 12 h. The samples were then pressed into pellets and sintered first at 1200 °C and then at 1500 °C for 12 h in air. X-ray powder diffraction measurements showed single phase patterns.

Magnetization curves $M(T)$ were established with a vibrating sample magnetometer. Samples were first zero field cooled before applying 0.6 T at 5 K. Measurements were carried out upon warning. The x-ray magnetic circular dichroism and x-ray absorption studies of these phases were performed systematically on the samples previously studied for their transport and magnetic properties. The structural characterization of the samples was realized by x-ray difraction, electron diffraction, and electron microscopy.[15] X-ray absorption spectra at Mn, Cr $L_{2,3}$ edge and Ln $M_{4,5}$ edges were recorded using circular polarized light at the Dragon beamline (ID12B) of the ESRF (Grenoble, France). To remove residual asymmetries, XAS and XMCD spectra were obtained by measuring the total yield signal at each photon energy at the opposite direction of the applied magnetic field of 0.55 T; spectra were then recorded for both light helicities with polarization between 80% and 90% (±5%) measured between 700 and 900 eV.[16] All the spectra were recorded after a zero field cooled process at $T=20$ K below the ferromagnetic Curie temperature of the samples. The samples were scraped *in situ* before each of the measurements. The base pressure in the spectrometer chamber was close to 10^{-10} mbar at the beginning of the experiment.

The SXMCD signals were corrected for partial circular polarization and are normalized to L_3 edge after background removal following a procedure described by Chen *et al.*[17]

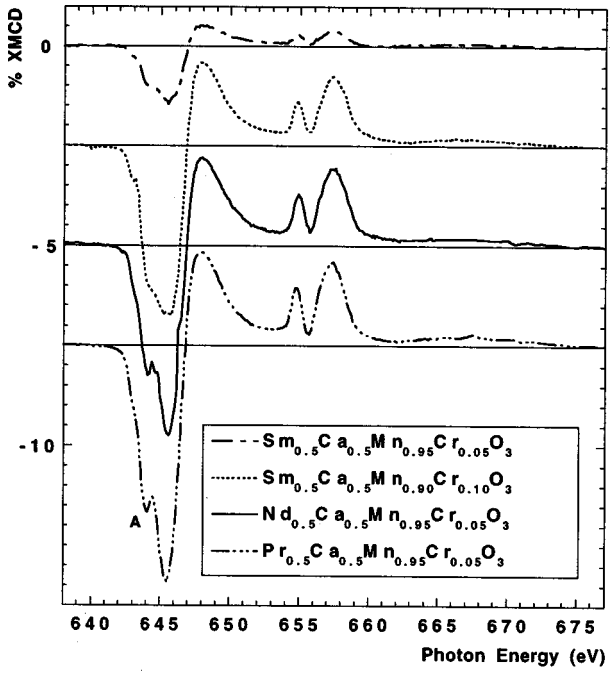

FIG. 1. SXMCD signal of $Ln_{0.5}Ca_{0.5}Mn_{0.95}Cr_{0.05}O_3$ (Ln=Pr, Nd, Sm) and $Sm_{0.5}Ca_{0.5}Mn_{0.90}Cr_{0.10}O_3$ at Mn $L_{2/3}$ edges at $T=20$ K. Shoulder *A* is likely due to $Mn^{4+}(3d^3)$ (Ref. 19).

III. RESULTS AND DISCUSSION

A. SXMCD at Mn $L_{2,3}$ edges

SXMCD at Mn $L_{2,3}$ edges of chromium doped rare earth manganites $Ln_{0.5}Ca_{0.5}Mn_{0.95}Cr_{0.05}O_3$ (Ln=Pr, Nd, Sm) and $Sm_{0.5}Ca_{0.5}Mn_{0.90}Cr_{0.10}O_3$ is shown in Fig. 1. The strong negative peak at about 645.5 eV already observed by Pellegrin[18] exhibits a shoulder *A*, which corresponds to the one observed on the XAS spectra. In agreement with a previous assignment,[19] shoulder *A* is likely due to $Mn^{4+}(3d^3)$. Earlier XAS measurements at the Mn *K* edge of the same samples showed that a formal charge of manganese is only slightly larger than $Mn^{3.5+}$ and considered equivalent to whatever the rare earth cation for a doping ratio is.[20] Thus, the variation of manganese formal charge cannot induce the observed changes in the SXMCD spectra at Mn $L_{2,3}$ edges for the various rare earths studied in the $Ln_{0.5}Ca_{0.5}Mn_{0.95}Cr_{0.05}O_3$ (Ln=Pr, Nd, Sm) series. Therefore, the reduction of the SXMCD signals when going from praseodyium to samarium manganite can be correlated to the decrease of the mean *A* site cation radius $\langle r_a \rangle$, which in turn can induce a reduction of the Mn–O–Mn angle already observed by x-ray and neutron diffraction. This reduction of the mean Mn–O–Mn angle reduces the double exchange mechanism and favors an antiferromagnetic ordering of the manganese subnetwork which reduces the SXMCD signal.

One also observe an increase of the magnetic moment carried by the manganese cation for $Sm_{0.5}Ca_{0.5}Mn_{1-x}Cr_xO_3$ ($x=0.05$ and 0.10). Introduction of chromium then causes spin realignment of part of Mn^{3+} to create a ferromagnetic manganese sublattice.

B. SXMCD at Cr $L_{2,3}$ edges

SXMCD at Cr $L_{2,3}$ edges of the same chromium doped rare earth manganites are shown in Fig. 2. The first qualitative but important information that can be drawn from XMCD signals is the relative orientation of both Cr and Mn magnetic subnetworks. The magnetic moment carried by the manganese cations, which is set parallel to the propagation vector of the soft x rays, was taken as reference. The Cr SXMCD spectra clearly show that Cr atoms possess a net moment antiparallel to the Mn moments as indicated by the positive SXMCD signal in the Cr L_3 range. Moreover, whatever the chromium ratio, SXMCD spectra show the same fine structure as that calculated for Cr^{3+} in octahedral crystal field symmetry with $10\,Dq=2$ eV.[21] These Cr $L_{2,3}$ edge atomic calculations confirm the Cr^{3+} formal charge which was already observed at Cr *K* edges.[20]

In the $Ln_{0.5}Ca_{0.5}Mn_{0.95}Cr_{0.05}O_3$ (Ln=Pr, Nd, Sm) series, the second important point is that SXMCD intensities at Cr $L_{2,3}$ edges vary in the same way as the ones observed at the Mn $L_{2,3}$ edge, resulting in agreement with the simultaneous presence of chromium and manganese atoms on the same perovskite *B* site. Thus, both magnetic sublattices interact with each other to give an average magnetic moment carried by the perovskite *B* site.

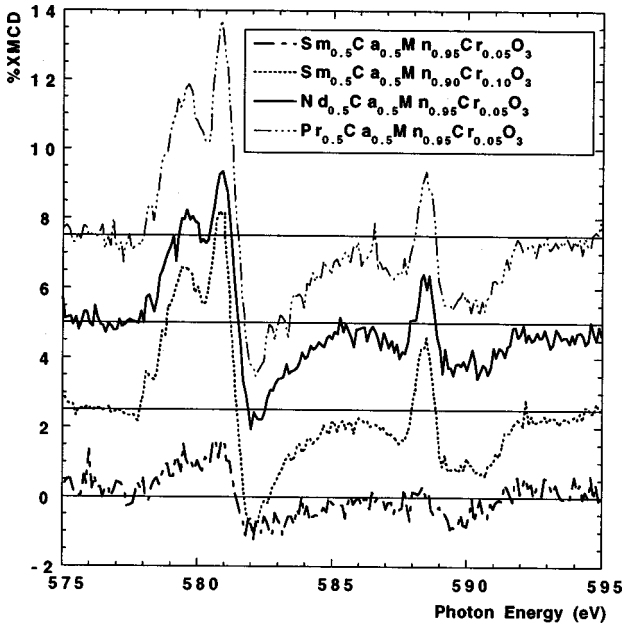

FIG. 2. SXMCD signal of $Ln_{0.5}Ca_{0.5}Mn_{0.95}Cr_{0.05}O_3$ (Ln=Pr, Nd, Sm) and $Sm_{0.5}Ca_{0.5}Mn_{0.90}Cr_{0.10}O_3$ at Cr $L_{2/3}$ edges at $T=20$ K.

Finally, for $Sm_{0.5}Ca_{0.5}Mn_{1-x}Cr_xO_3$ ($x=0.05$ and 0.10), one also observed an increase of the magnetic moment carried by the chromium cation with the doping ration so that an increase of the ferromagnetic ordering on the chromium sublattice, as already observed on manganese sublattice, can be deduced from XMCD measurements.

C. SXMCD at rare earth $M_{4,5}$ edges

The SXMCD signal at rare earth $M_{4,5}$ edges of $Ln_{0.5}Ca_{0.5}Mn_{0.95}Cr_{0.05}O_3$ (Ln=Pr, Nd) and $Sm_{0.5}Ca_{0.5}Mn_{0.90}Cr_{0.10}O_3$ are plotted in Fig. 3(a), whereas the SXMCD integrated signals are shown in Fig. 3(b). In comparison, the respective rare earth edge energies were substracted: 929 eV for praseodymium, 980 eV for neodymium, and 1083 eV for samarium at the M_5 edge. Taking as reference atomic calculations of the dichroic signals at $M_{4,5}$ edges of trivalent rare earth ions due to Goedkoop,[22] Pr and Nd magnetic sublattices appear aligned parallel to the Mn moments, whereas samarium magnetic sublattice is aligned in the reverse way antiparallel to the Mn moments.

D. Sum rules application

By applying a sum rule,[23] one should be able to estimate the operators of the orbital magnetic moment $\langle L_z \rangle$ and the operators of the spin magnetic moment $\langle S_z \rangle$ for each probed element and edge.

In the case of manganese and chromium oxides, the spin-orbit splitting of the core hole is not large enough to prevent mixing of the J contributions to the L_3 and L_2 edges[24] such that an error in the determination of $\langle S_z \rangle$ as large as 200% has been shown by the multiplet calculations.[25] So, one can only give (Table I) an estimation of the orbital magnetic moment:

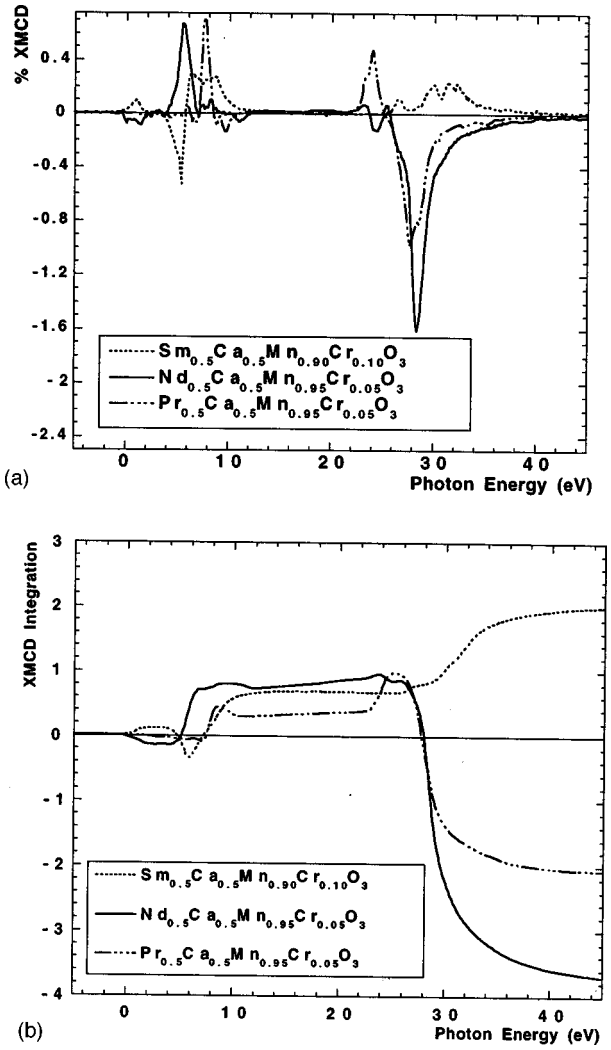

FIG. 3. (a) SXMCD signal at rare earth $M_{4,5}$ edges of $Ln_{0.5}Ca_{0.5}Mn_{0.95}Cr_{0.05}O_3$ (Ln=Pr, Nd) and $Sm_{0.5}Ca_{0.5}Mn_{0.90}Cr_{0.10}O_3$ at $T=20$ K. Rare earth M_5 edge energy was substracted: 929 eV for praseodymium, 980 eV for neodymium, and 1083 eV for samarium. (b) Integrated SXMCD signal at rare earth $M_{4,5}$ edges of $Ln_{0.5}Ca_{0.5}Mn_{0.95}Cr_{0.05}O_3$ (Ln=Pr, Nd) and $Sm_{0.5}Ca_{0.5}Mn_{0.90}Cr_{0.10}O_3$ at $T=20$ K.

$$\langle L_z^{3d} \rangle = -\frac{4\int_{L_3+L_2}(\mu^+ - \mu^-)dE}{3\int_{L_3+L_2}(\mu^+ + \mu^-)dE}$$

in agreement with previous calculations[18,19] where n_{3d} is the $3d$ electron occupation number of the considered cation, L_3+L_2 denote the integration ranges, and $\mu^+(\mu^-)$ is the absorption cross sections of the sample when the magnetic field is applied parallel (antiparallel) to the propagation direction of the x rays with fixed circular polarization. Because of the weakness of the SXMCD signal, applying the sum rule to the Cr $L_{2,3}$ edges provides a more rough estimation of the orbital magnetic moment $\langle L_z^{3d} \rangle$, which turns out to be of the same order of magnitude as the one found in the case of the manganese $L_{2,3}$ edge. These orbital magnetic moment values correpond to a quenched orbital contribution as usual in the case of transition metal.

In the case of rare earth $M_{4,5}$ edges, the estimation of the orbital magnetic moments and spin magnetic moments are

TABLE I. Orbital and spin magnetic moment carried by manganese $3d$ shell and rare earth $4f$ shell.

Compounds	Manganese $\langle L_z^{3d}\rangle$ μ_B	Chromium $\langle L_z^{3d}\rangle$ μ_B	Rare earth $\langle L_z^{4f}\rangle$ μ_B	Rare earth $\langle S_z^{4f}\rangle$ μ_B	Rare earth $\langle M_z^{4f}\rangle$ μ_B
$Pr_{0.5}Ca_{0.5}Mn_{0.95}Cr_{0.05}O_3$	$+3.0\times10^{-2}$	-4.9×10^{-2}	-0.9×10^{-1}	$+0.3\times10^{-1}$	$+3\times10^{-2}$
$Nd_{0.5}Ca_{0.5}Mn_{0.95}Cr_{0.05}O_3$	$+5.6\times10^{-2}$	-2.0×10^{-2}	-1.5×10^{-1}	$+1.1\times10^{-1}$	-7×10^{-2}
$Sm_{0.5}Ca_{0.5}Mn_{0.95}Cr_{0.05}O_3$	-0.3×10^{-2}	-1.0×10^{-2}	not measured	not measured	not measured
$Sm_{0.5}Ca_{0.5}Mn_{0.90}Cr_{0.10}O_3$	$+6.6\times10^{-2}$	-1.0×10^{-2}	$+0.4\times10^{-1}$	-0.1×10^{-1}	-2×10^{-2}

also given in Table I. The estimation of the spin magnetic moment is indirectly given by the second sum rule

$$\frac{\langle L_Z\rangle}{2\langle S_e\rangle}=\frac{2\int_{M_4+M_5}(\mu^+-\mu^-)dE}{2\int_{M_5}(\mu^+-\mu^-)dE-3\int_{M_4}(\mu^+-\mu^-)dE},$$

where μ^+ and μ^- are always the absorption cross sections of the sample when the magnetic field is applied parallel and antiparallel, respectively, to the propagation direction of the x rays with fixed circular polarization. M_4 and M_5 denote the integration ranges and $\langle S_e\rangle\equiv\langle S_z\rangle+3\langle T_z\rangle$, where $\langle T_z\rangle$ is the expectation value of the magnetic dipole operator which describes correlations between the spin and position of each electron and $\langle S_z\rangle$ is the expected spin magnetic moment. Hence, whereas the first sum rule provides a direct estimation of $\langle L_z^{4f}\rangle$, the estimation of $\langle S_z^{4f}\rangle$ from the second sum rule requires the knowledge of $\langle T_z\rangle$. $\langle T_z\rangle$ is difficult to measure but theoretical values of the ratio $\langle T_z\rangle/\langle S_z\rangle$ for the rare earths have been published by Carra *et al.*[23] $\langle T_z\rangle/\langle S_z\rangle$ is estimated at 0.58 for Pr^{3+} ($N_{4f}=2$, $L=5$, $S=1$), 0.14 for Nd^{3+} ($N_{4f}=3$, $L=6$, $S=3/2$), and 0.23 for Sm^{3+} ($N_{4f}=5$, $L=5$, $S=5/2$). Hence, as $m_{\rm orb}=-\langle L_z^{4f}\rangle\mu_B$ and $m_{\rm spin}=-2\langle S_z^{4f}\rangle$, one can estimate the total magnetic moment equal to $m_{\rm orb}+m_{\rm spin}$ (Table I). $\langle L_z\rangle$ and $\langle S_z\rangle$ are antiparallel and nearly compensate each other explaining the weak total magnetic moment. The weak magnitude of the total magnetic moment is in agreement with the one calculated from neutron diffraction experiments for Nd^{3+} and Pr^{3+} ($M_{\rm Ln}^{3+}\approx0.45\mu_B$ at 4 K) on $Ln_{0.7}A_{0.3}MnO_3$.[26,27] Taking into account that the spin-orbit splitting of the core hole is certainly not large enough to prevent a mixing of the J contributions to the M_5 and M_4 edges, atomic calculations of Ln^{3+} would be necessary to obtain the moment by scaling as it were done for Er^{3+}.[28] The sign of the operators of the orbital magnetic moment $\langle L_z\rangle$ and of the spin magnetic moment $\langle S_z\rangle$ for the probed rare earth is linked to the qualitative information provided by SXMCD concerning the orientation of the rare earth magnetic moment parallel or antiparallel to the ferromagnetic manganese sublattice.

IV. MODEL OF MAGNETIC ORDERING IN DOPED MANGANITES

A. Rare earth magnetic moments

To propose a magnetic model for the rare earth in the manganites, one must take into account that previous SXMCD work on $Nd_{0.72}Ba_{0.28}MnO_3$[19] has shown the existence of a flipping of the neodymium magnetic sublattice depending on the applied magnetic field. Neutron diffraction studies have estimated a weak ferromagnetic moment to $0.4(5)\mu_B$ on Pr ions and parallel to the Mn moment[27] for $Pr_{0.7}Ca_{0.3}MnO_3$ but, antiparallel to the Mn moment in the case of Nd ions—with the same order of magnitude—for $Nd_{0.72}Ba_{0.28}MnO_3$.[26] Thus the rare earth magnetic sublattice can be seen as a distribution of magnetic moments on a cone with the main axis aligned in the direction of manganese magnetic moments. The axis of this conic distribution of rare earth magnetic moments would then be parallel or antiparallel to the ferromagnetic manganese sublattice, depending on the sign of the magnetic exchange interaction, i.e., depending on the rare earth nature. The statistical distribution of the rare earth cation and the mismatch on the perovskite A site, inducing frustration in the magnetic interaction, would be at the origin of the weak coupling and change of orientation of rare earth magnetic moments.

Recent SXMCD measurements at the Pr $M_{4,5}$ edge on $Pr_{0.7}Sr_{0.3}MnO_3$ thin film[29] showing an increase of the SXMCD signal with the increase of the applied magnetic field, could be interpreted also as the result of the reduction of the cone angle provided that the magnetic domain saturation occurs in low magnetic field. Increase of the applied magnetic field will tend to align the Pr moment parallel to the direction of the propagation vector of the soft x rays, thus reducing the cone angle around the applied magnetic field direction.

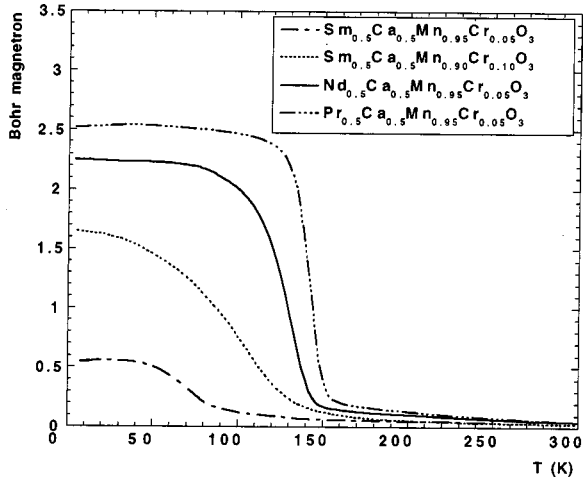

FIG. 4. Thermal variation under 0.6 T of the magnetization of the samples $Ln_{0.5}Ca_{0.5}Mn_{0.95}Cr_{0.05}O_3$ (Ln=Pr, Nd, Sm) and $Sm_{0.5}Ca_{0.5}Mn_{0.90}Cr_{0.10}O_3$.

TABLE II. SXMCD asymmetries at 645.5 eV for Mn $L_{2,3}$ edge at 580.7 eV for Cr $L_{2,3}$ edge and at M_4 edge for the various rare earths studied and samples calibrated.

Compounds	Mn SXMCD asymmetry (%)	Cr SXMCD asymmetry (%)	Weighted asymmetry on *B* site pervoskite	Ln SXMCD asymmetry (%)
$Pr_{0.5}Ca_{0.5}Mn_{0.95}Cr_{0.05}O_3$	−5.9	+6.2	−5.2(9)	+0.7
$Nd_{0.5}Ca_{0.5}Mn_{0.95}Cr_{0.05}O_3$	−4.7	+4.3	−4.2(5)	+0.7
$Sm_{0.5}Ca_{0.5}Mn_{0.95}Cr_{0.05}O_3$	−1.4	+1.9	−1.2(3)	/
$Sm_{0.5}Ca_{0.5}Mn_{0.90}Cr_{0.10}O_3$	−4.1	+5.7	−3.1(2)	−0.5

Nevertheless, this work confirms that, except for lanthanum, rare earth cations carry a magnetic moment due to $4f$ electrons. However, the existence of magnetic moments on the rare earth cation seems to be uncorrelated with magnetoresistance properties which take place at higher temperature than the estimated Curie temperature of the magnetic ordering of the rare earth sublattice. This result was already pointed out in the SXMCD study of $Nd_{0.72}Ba_{0.28}MnO_3$, where the observed flipping of the neodymium magnetic moment with increasing applied magnetic field did not affect the magnetoresistance properties.

However, magnetization measurement recorded at 0.6 T for various samples studied by SXMCD is shown in Fig. 4. Considering the SXMCD results, one can now better understand the variations of the saturation magnetization at 5 K. The total magnetization is the addition of manganese, chromium, and rare earth moments. Table II presents the SXMCD asymmetries $(\mu_+ - \mu_-)/(\mu_+ + \mu_-)$ at 645.5 eV for Mn $L_{2,3}$ edge, at 580.7 eV for Cr $L_{2,3}$ edge and at the rare earth M_4 edge. Contrary to the magnetic multilayers system,[30] it is difficult to determine an average magnetic moment on the pervoskite *B* site by comparison with a reference manganite because of the intrinsic properties of the manganese–oxygen bonds.[31] In manganeses oxides, the magnetization depends on the Mn–O distance and on the O–Mn–O angle which is linked to the mean *A* site cation radius $\langle r_a \rangle$, which induces a reduction of the O–Mn–O angle and on the filling of the $Mn(3d)-O(2p)$ molecular orbitals, i.e., on the Mn^{4+}/Mn^{3+} ratio. Nevertheless, considering an average magnetic moment on the *B* site estimated by the sum of the weighted asymmetries found at the Cr and Mn $L_{2,3}$ edge, these asymmetries show a qualitative agreement with the variations of the total magnetization which decreases from Pr to Sm. Moreover, one should take into account the rare earth magnetic contribution to the total moment which can be parallel or antiparallel to the manganese magnetic moment. Then, by adding to the average magnetic moments on the perovskite *B* site, a positive magnetic moment for $Nd_{0.5}Ca_{0.5}Mn_{0.95}Cr_{0.05}O_3$ and a negative magnetic moment for $Sm_{0.5}Ca_{0.5}Mn_{0.90}Cr_{0.10}O_3$ in agreement with the relative orientation of the observed magnetic moment carried by the perovskite *A* site, one can find a second reason for the variation of the total magnetization at low temperature between these two samples.

Finally, the transition width from the paramagnetic to the ferromagnetic state increases drastically with the reduction of the mean *A* site cation radius $\langle r_a \rangle$ (Fig. 4). Such a result is also usually observed in the CMR rare earth manganites upon increase of the applied magnetic field. This is likely due to the distribution of magnetic moments induced by a variable spread in energy of magnetic polarons.[11]

V. CONCLUSION

Existence and orientation of local magnetic moments of specific atoms have been obtained from soft-x-ray magnetic dichroim measurements (SXMCD) in doped CMR manganites. Qualitative information about the magnetic moment magnitudes of the probed cations has also been extracted from the spectra. Soft XMCD of the doping transition metals appears to be a unique technique to give informations about the magnetic behavior of elements in weak amounts inside complex materials. However, the detailed interpretation of the data will require thoroughful multiplet calculations, especially for the estimation of the spin contribution to the dichroic signal.

The correlation between the total magnetization and the soft XMCD measurements allows us to better understand the magnetic ordering inside the transition metal doped CMR rare earth manganites.

The chromium magnetic sublattice appears to be antiparallel to the manganese magnetic sublattice taken as a reference and a reversal of Sm magnetic moments with respect to Pr and Nd moments has been observed. The small magnitudes of the total moment of Pr and Nd observed by neutron diffraction are in agreement with the small amplitude of the total magnetic contribution found in SXMCD spectra and let us think of a conic distribution of rare earth magnetic moments around the direction of the applied magnetic field ($H = 0.6\,\mathrm{T}$). Such a result may account for the easy reversal of the Nd magnetic moments upon the increase of the applied magnetic field observed in the study of the $Nd_{0.72}Ba_{0.28}MnO_3$ CMR manganite.

Further experiments will be necessary to determine the ordering temperature of the chromium and rare earths magnetic sublattices to correlate magnetic moment carried by chromium with magnetoresistance properties.

[1] P. Rudolf, F. Sette, L. H. Tjeng, G. Meigs, and C. T. Chen, J. Magn. Magn. Mater. **109**, 109 (1992); C. Giorgetti *et al.*, Phys. Rev. B **48**, 17, 12732 (1993); J. Vogel, A. Fontaine, V. Cros, F. Petroff, J. P. Kappler, G. Krill, A. Rogalev, and J. Goulon, Phys. Rev. B **55**, 3663 (1997); W. F. Pong, Y. K. Chang, M. H. Su, P. K. Tseng, H. J. Lin, G. H. Ho, K. L. Tsang, and C. T. Chen, *ibid.* **55**, 11409 (1997); A. Kimura, S. Suga, T. Shishidou, S. Imada, T. Muro, S. Y. Park, T. Miyahara, T. Kaneka, and T. Kanomata, *ibid.* **56**, 6021 (1997); G. Schutz, P. Fischer, E. Goering, K.

Attekofer, D. Ahlers, and W. Rossl, Synchrotron Radiat. News **10**, 13–26 (1997).
[2] B. Raveau, A. Maignan, and C. Martin, J. Solid State Chem. **130**, 162 (1997); A. Barnabe, A. Maignan, M. Hervieu, F. Damay, C. Martin, and B. Raveau, Appl. Phys. Lett. **71**, 3907 (1998).
[3] R. M. Kuster, J. Singleton, D. A. Keon, R. M. Greedy, and W. Hayes, Physica B **155**, 362 (1989); R. Von Hemmolt, J. Wecker, B. Holzapfel, L. Schultz, and K. Samwer, Phys. Rev. Lett. **71**, 2331 (1993); H. L. Ju, C. Kwon, Q. Li, R. L. Greene, and T. Venkaten, Appl. Phys. Lett. **65**, 2108 (1994); A. Maignan, Ch. Simon, V. Caignaert, and B. Raveau, Solid State Commun. **96**, 623 (1995); R. Mahesh, R. Mahendiran, A. K. Raychaudhury, and C. N. R. Rao, J. Solid State Chem. **114**, 297 (1995); S. Jin, H. M. O'Bryan, T. H. Tiefel, M. McCormack, and W. W. Rhodes, Appl. Phys. Lett. **66**, 382 (1995).
[4] C. Zener, Phys. Rev. **82**, 403 (1951); P. W. Anderson and H. Hasegawa, *ibid.* **100**, 975 (1955); P. G. De Gennes, *ibid.* **118**, 141 (1960).
[5] A. J. Millis, P. B. Litlewood, and B. I. Shraiman, Phys. Rev. Lett. **74**, 5144 (1995); A. J. Millis, B. I. Shraiman, and R. Mueller, *ibid.* **77**, 175 (1996).
[6] V. Caignaert, E. Suard, A. Maignan, Ch. Simon, and B. Raveau, J. Magn. Magn. Mater. **153**, L260 (1996); J. L. Garcia-Munoz, M. Suaidi, J. Fontcuberta, and J. Rodriguez-Carvajal, Phys. Rev. B **55**, 34 (1997).
[7] P. Dai, J. Zhang, H. A. Mook, S. H. Liou, P. A. Dowben, and E. W. Plummer, Phys. Rev. B **54**, R3694 (1996).
[8] C. Meneghini, R. Cimino, S. Pascarelli, S. Mobilio, C. Raghu, and D. D. Sarma, Phys. Rev. B **56**, 3520 (1997); C. H. Booth, F. Bridges, G. H. Kwei, J. M. Lawrence, A. L. Cornelius, and J. J. Neumeier, Phys. Rev. Lett. **80**, 853 (1998).
[9] O. Toulemonde, F. Millange, F. Studer, B. Raveau, J.-H. Park, and C-T. Chen, J. Phys.: Condens. Matter **11**, 109 (1999).
[10] F. Studer, O. Toulemonde, V. Caignaert, P. Srivastava, J. B. Goedkoop, and N. Brookes, J. Phys. IV **7**, C2-529 (1997).
[11] J. M. De Teresa, M. R. Ibarra, P. A. Algarabel, C. Ritter, C. Marquina, J. Blasco, J. Garcia, A. del Moral, and Z. Arnold, Nature (London) **386**, 256 (1997).
[12] P. S. Anil Kumar, P. A. Joy, and S. K. Date, J. Phys.: Condens. Matter **10**, L269 (1998).
[13] J. H. Park, E. Vescovo, H. J. Kim, C. Kwon, R. Ramesh, and T. Venkatesan, Nature (London) **392**, 794 (1998).
[14] S. Satpathy, Z. S. Popovic, and F. R. Vukajlovic, Phys. Rev. Lett. **76**, 960 (1996).
[15] A. Barnabé, M. Hervieu, C. Martin, A. Maignan, and B. Raveau, J. Mater. Chem. **8**, 1405 (1998).
[16] M. Drescher, G. Schnell, U. Kleineberg, H. J. Stock, N. Muller, U. Heinzmann, and N. B. Brookes, Rev. Sci. Instrum. **68**, 1939 (1996).
[17] C. T. Chen, Y. U. Idzerda, H-J. Lin, N. V. Smith, G. Meigs, E. Chaban, G. H. Ho, E. Pellegrin, and F. Sette, Phys. Rev. Lett. **75**, 152 (1995).
[18] E. Pellegrin *et al.*, J. Phys. IV **7**, C2-405 (1997).
[19] O. Toulemonde *et al.*, J. Magn. Magn. Mater. **190**, 307 (1998).
[20] O. Toulemonde, F. Studer, A. Barnabé, A. Maignan, C. Martin, and B. Raveau, Eur. Phys. J. B **4**, 159 (1998).
[21] G. Van Der Laan and B. T. Thole, Phys. Rev. B **43**, 13401 (1991).
[22] J. B. Goedkoop, thesis, University of Nijmegen (1989).
[23] B. T. Thole *et al.*, Phys. Rev. Lett. **68**, 1943 (1992); P. Carra *et al.*, *ibid.* **70**, 694 (1993).
[24] Y. Teramura, A. Tanaka, and T. Jo, J. Phys. Soc. Jpn. **65**, 1053 (1996).
[25] E. Pellegrin (private communication).
[26] D. E. Cox, P. G. Radaelli, M. Marezio, and S. W. Cheong, Phys. Rev. B **57**, 3305 (1998).
[27] F. Fauth, E. Suard, C. Martin, and F. Millange, Physica B **241**, 427 (1998).
[28] L. M. Garcia, S. Pizzini, J. P. Rueff, J. Vogel, R. M. Galera, A. Fontaine, J. P. Kappler, G. Krill, and J. B. Goedkoop, J. Appl. Phys. **79**, 6497 (1996).
[29] O. Toulemonde, F. Studer, J. Wolfman, B. Mercey, Ch. Simon, and J. Goedkoop (unpublished).
[30] Y. U. Idzerda, L. H. Tjeng, H. J. Lin, C. J. Guttierrez, G. Meigs, and C. T. Chen, Phys. Rev. B **48**, 4144 (1993); S. Andrieu, E. Foy, H. Fischer, M. Alnot, F. Chevrier, G. Krill, and M. Piecuch, *ibid.* **58**, 8210 (1998); M. A. Tomaz, W. J. Antel, Jr., W. L. O'Brien, and G. R. Harp, *ibid.* **55**, 3716 (1997).
[31] J. L. Garcia-Munoz, J. Fontcuberta, B. Martinez, A. Seffar, S. Pignol, and X. Obradors, Phys. Rev. B **55**, R668 (1997).